

Durham Research Online

Deposited in DRO:

23 April 2019

Version of attached file:

Accepted Version

Peer-review status of attached file:

Peer-reviewed

Citation for published item:

Lechleitner, Franziska A. and Lang, Susan Q. and Haghypour, Negar and McIntyre, Cameron and Baldini, James U.L. and Prufer, Keith M. and Eglinton, Timothy I. (2019) 'Towards organic carbon isotope records from stalagmites: coupled d13C and 14 C analysis using wet chemical oxidation.', *Radiocarbon*, 61 (3). pp. 749-764.

Further information on publisher's website:

<https://www.cambridge.org/core/journals/radiocarbon/article/towards-organic-carbon-isotope-records-from-stalagmites-coupled-13c-and-14c-analysis-using-wet-chemical-oxidation/7326D57C0DF9D89C352D8DB3F152ABCF>

Publisher's copyright statement:

This article has been published in a revised form in *Radiocarbon* [<https://doi.org/10.1017/RDC.2019.35>]. This version is free to view and download for private research and study only. Not for re-distribution, re-sale or use in derivative works. © 2019 by the Arizona Board of Regents on behalf of the University of Arizona

Additional information:

Use policy

The full-text may be used and/or reproduced, and given to third parties in any format or medium, without prior permission or charge, for personal research or study, educational, or not-for-profit purposes provided that:

- a full bibliographic reference is made to the original source
- a [link](#) is made to the metadata record in DRO
- the full-text is not changed in any way

The full-text must not be sold in any format or medium without the formal permission of the copyright holders.

Please consult the [full DRO policy](#) for further details.

1 **Towards organic carbon isotope records from stalagmites: coupled $\delta^{13}\text{C}$ and ^{14}C analysis**
2 **using wet chemical oxidation**

3

4 Franziska A. Lechleitner^{1,2,3*}, Susan Q. Lang⁴, Negar Haghypour^{2,5}, Cameron McIntyre⁶, James
5 U.L. Baldini³, Keith Prufer⁷, Timothy I. Eglinton²

6

7 ¹Department of Earth Sciences, University of Oxford, South Parks Road, Oxford OX1 3AN,
8 UK

9 ²Department of Earth Sciences, ETH Zurich, Sonneggstrasse 5, 8092 Zurich, Switzerland

10 ³Department of Earth Sciences, University of Durham, Science Site, Durham DH1 3LE, UK

11 ⁴School of the Earth, Ocean, and Environment, University of South Carolina, 701 Sumter
12 Street, EWS 617, Columbia SC 29208, USA

13 ⁵Laboratory of Ion Beam Physics, Department of Physics, ETH Zurich, Otto-Stern-Weg 5, 8093
14 Zurich, Switzerland

15 ⁶Scottish Universities Environmental Research Centre (SUERC), Rankine Avenue, East
16 Kilbride G75 0GF, UK

17 ⁷Department of Anthropology, University of New Mexico, Albuquerque, NM 87106, USA

18

19 Keywords: organic matter, stalagmite, carbon isotopes, bomb spike

20 *corresponding author: franziska.lechleitner@earth.ox.ac.uk

21

22 **ABSTRACT**

23 Speleothem organic matter can be a powerful tracer for past environmental conditions and karst
24 processes. Carbon isotope measurements ($\delta^{13}\text{C}$ and ^{14}C) in particular can provide crucial
25 information on the provenance and age of speleothem organic matter, but are challenging due
26 to low concentrations of organic matter in stalagmites. Here, we present a method development
27 study on extraction and isotopic characterization of speleothem organic matter using a rapid
28 procedure with low laboratory contamination risk. An extensive blank assessment allowed us
29 to quantify possible sources of contamination through the entire method. Although blank
30 contamination is consistently low ($1.7 \pm 0.34 - 4.3 \pm 0.86 \mu\text{g C}$ for the entire procedure),
31 incomplete sample decarbonation poses a still unresolved problem of the method, but can be
32 detected when considering both $\delta^{13}\text{C}$ and ^{14}C values. We test the method on five stalagmites,
33 showing reproducible results on samples as small as $7 \mu\text{g C}$ for $\delta^{13}\text{C}$ and $20 \mu\text{g C}$ for ^{14}C .
34 Furthermore, we find consistently lower non-purgeable organic carbon (NPOC) ^{14}C values
35 compared to the carbonate ^{14}C over the bomb spike interval in two stalagmites from Yok Balum
36 Cave, Belize, suggesting overprint of a pre-aged or even fossil source of carbon on the organic
37 fraction incorporated by the stalagmites.

Commented [SSE1]: I think that this is a really
fundamental observation

38 **INTRODUCTION**

39 Organic matter entrapped in speleothem carbonate is increasingly recognized as a promising
40 tool for the reconstruction of past ecosystem and climate change (Blyth et al., 2016; Bosle et
41 al., 2014; Heidke et al., 2018; Perrette et al., 2015; Quiers et al., 2015). Organic carbon (OC)
42 primarily originates from the overlying soil and karst system from which it is transported into
43 caves by vadose water, or from microbial production within the cave (Blyth et al., 2016). Other
44 sources of OC in cave systems include airborne material, generally limited to areas near the
45 cave entrances, and compounds derived from cave-dwelling animals and insects, which can
46 constitute a major source of OC if large animal populations are present (Blyth et al., 2008). The
47 portion of OC stemming from the surface is argued to be dominant in most karst systems (Baker
48 and Genty, 1999; Perrette et al., 2015; Quiers et al., 2015; Shabarova et al., 2014), but
49 substantial reworking of OC is generally observed (Birdwell and Engel, 2010; Einsiedl et al.,
50 2007; Lechleitner et al., 2017; Shabarova et al., 2014). Nevertheless, OC incorporated in
51 stalagmites is considered a potentially very sensitive proxy for surface environmental
52 conditions (Blyth et al., 2016, 2008).

53 Isotopic studies on carbon can provide insight into provenance, processing, and age of organic
54 matter in environmental matrices. Stable carbon isotope ratios ($\delta^{13}\text{C}$) in biogenic samples are
55 generally strongly fractionated by metabolic processes. Higher plants utilizing the C3 carbon
56 fixation pathway exhibit very negative $\delta^{13}\text{C}$ values (-32 to -22‰), whereas C4 plants fractionate
57 less strongly (-16 to -10‰) (Vogel, 1980). Radiocarbon (^{14}C), in contrast, provides a measure
58 of the age of OC analysed, indicating its recalcitrance and turnover time.

59 The conventional understanding is that OC incorporated in stalagmites is not directly affected
60 by the addition of ^{14}C -dead carbon from limestone dissolution (Blyth et al., 2017), and may
61 thus provide important constraints on drivers of the karst carbon cycle, and on (past) surface
62 conditions.

63 Because of the very low amounts of organic carbon found in stalagmites embedded in a matrix
64 virtually exclusively derived of carbonate, large sample sizes typically need to be processed for
65 analysis and careful treatments are needed to remove inorganic carbon and other interferences.
66 Both increase the potential for contamination through laboratory procedures, rendering such
67 measurements challenging (Wynn and Brocks, 2014). Moreover, the effect of large sample
68 sizes on their chronological assessment needs to be considered, e.g., through sampling along
69 growth layers where possible (fast growing stalagmites). Thus far, a few studies on $\delta^{13}\text{C}$ in non-
70 purgeable organic carbon (NPOC) incorporated in stalagmites have been conducted (Blyth et
71 al., 2013b, 2013a) using an approach based on acid digestion of stalagmite samples to remove
72 inorganic carbon from CaCO_3 , followed by oxidation of the carbon remaining in the solution
73 to CO_2 , from which $\delta^{13}\text{C}$ can then be determined. Their results show that accurate and
74 reproducible $\delta^{13}\text{C}$ measurements are possible from stalagmites, using relatively small sample

75 amounts (100-200 mg CaCO₃). To our knowledge, the only published studies on stalagmite OC
76 ¹⁴C to date concentrate on the use of speleothems with high OC concentrations for dating
77 purposes (e.g., Blyth et al., 2017; Borsato et al., 2000; Genty et al., 2011). Thus far, however,
78 there have been no reported ¹⁴C measurements on stalagmite NPOC, likely because sample size
79 requirements are substantially greater, with attendant increases in procedural blanks and other
80 analytical uncertainties. The latter limitation is partly alleviated by recent developments in
81 accelerator mass spectrometry that permit analysis of small (<20 µg C) samples (Fahrni et al.,
82 2013; Ruff et al., 2007). Here, we describe a suite of experiments conducted to develop an
83 extraction and oxidation procedure that builds on prior developments (Lang et al., 2016, 2013,
84 2012), and show results from its application for studies of both δ¹³C and ¹⁴C of NPOC preserved
85 in stalagmites. After testing the method on three stalagmite samples, we applied it on two well-
86 dated stalagmites from Yok Balum Cave, Belize (YOK-G and YOK-I). Both stalagmites were
87 previously sampled for high-resolution inorganic ¹⁴C (Lechleitner et al., 2016a; Ridley et al.,
88 2015), revealing a very clear imprint of bomb ¹⁴C in the carbonate phase. Because of high
89 growth rates in these stalagmites, enough sample material was available to analyse NPOC ¹⁴C
90 before and after the bomb pulse, providing an opportunity to study the organic carbon cycle in
91 cave systems from a ¹⁴C perspective for the first time.

92

93 MATERIALS

94 Stalagmite Samples

95 Five different stalagmites of different provenance, age, and mineralogy were used for this
96 preliminary study (Table 1, Fig. 1). Stalagmites are prone to OC contamination, either from
97 improper handling or outside influences (Wynn and Brocks, 2014). Therefore, any method
98 attempting to extract a primary NPOC signal from these samples needs to consider and
99 eliminate the possibility of sample contamination, particularly on the stalagmite surface. In this
100 study, two methods for the removal of contaminated surfaces were applied. The test stalagmites
101 TSAL, BB2, and YOK-K were available as discrete sample pieces. In this case, the entire
102 sample was leached with 1N HCl to remove about 1g of CaCO₃ (5-20% of total mass) from all
103 surfaces. After leaching, the samples were washed three times with ultrapure water and dried
104 in an oven at 60°C, before being powdered to homogeneity using an agate mortar pre-cleaned
105 with methanol and dichloromethane. All sample powders were stored in pre-combusted glass
106 vials with acid-washed Teflon caps (storage time varied from days to months, depending on the
107 sample).

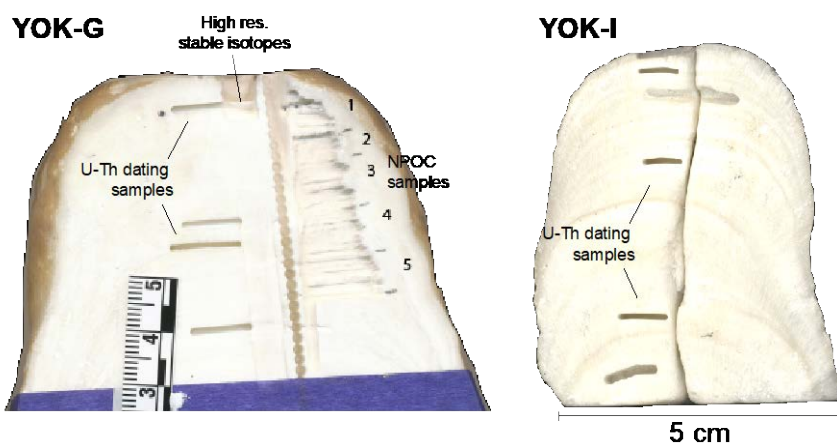
108 For stalagmites YOK-I and YOK-G, smaller samples were drilled from specific depths to
109 capture the bomb spike interval. For YOK-I, this was achieved by drilling samples using a
110 hand-held drill (Dremel 4000) equipped with newly purchased diamond-coated drill bits. The
111 drill bits were pre-cleaned by extracting them three times using methanol, dichloromethane,

Commented [SSE2]: Could we elaborate a bit here?
Listing at least the cave here would be useful

112 and ultrapure water, and dried in an oven at 60°C overnight. Before drilling, dust and particles
 113 were removed from the stalagmite surface using compressed air, and the top ~ 1mm was
 114 removed using a separate drill bit and discarded. For YOK-G, a new Kodiak carbide end mill
 115 was used on a Sureline micromill, and the drill bit was cleaned with HPLC-grade methanol and
 116 ultrapure water before and in between sampling. Dust and powder was removed from the
 117 stalagmite surface before and between sampling, and the powdered samples from YOK-G were
 118 shipped to the laboratory at ETH Zurich in sterile microcentrifuge vials.
 119

Sample ID	Cave	Region	Sampled age	Mineralogy	Colour	Notes
TSAL	Tskaltubo	Caucasus	40 kyr BP	calcite	clear white	
BB2	Blessberg	Germany	6 kyr BP	calcite	brownish	
YOK-K	Yok Balum	Central America	n.d.	aragonite	brown and grey layers	
YOK-I			1910-1980 CE	aragonite	white with grey layers	sampling over bomb spike interval
YOK-G			1940-1980 CE	aragonite	clear white	

120 **Table 1.:** Details of the stalagmites used. Sample ages are given in kyr BP (thousands of years
 121 before present, with the present defined as 1950 CE), or as CE, i.e., Common Era.
 122



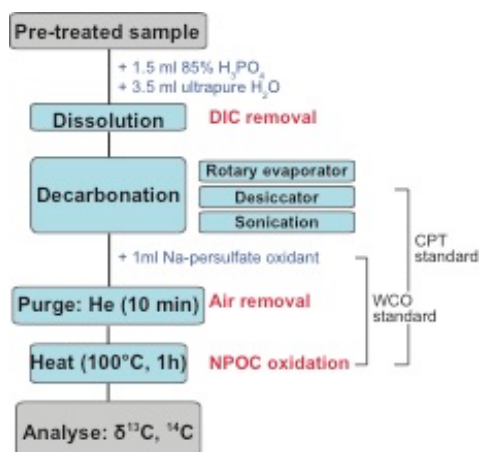
123 **Fig. 1.:** Top sections of stalagmites YOK-G and YOK-I from Yok Balum Cave, Belize. In this
 124 study, the bomb spike interval was targeted for isotopic characterization of the organic matter
 125 entrapped in stalagmite carbonate. For sample YOK-G, the tracks left by drilling for NPOC
 126 analysis are visible.
 127

128

129 METHODS

130 Decarbonation

131 Aliquots of the powdered stalagmites were transferred to pre-combusted 12 ml borosilicate
 132 Exetainer screw-capped vials with butyl rubber septa (Labco, High Wycombe, UK).
 133 Decarbonation of the samples to remove inorganic carbonate proceeded by adding 1.5 ml of
 134 85% H₃PO₄ (puriss. grade), followed by 3.5 ml of ultrapure water (18.2 MΩ and ≤ 5 ppb TOC)
 135 (Fig. 2). Acid and water were added stepwise and the vials were briefly vortexed in between to
 136 ensure complete submersion of the CaCO₃. The samples were then left to dissolve on the
 137 laboratory bench (room temperature: 23°C) covered with clean aluminium foil or acid-washed
 138 vial caps. Because traditional CaCO₃ dissolution protocols (i.e., purging the solution with He
 139 for 5-10 min) resulted in residual inorganic carbon contributions in the final extracts (as
 140 indicated by high δ¹³C values, ~ -9‰), we tested several approaches to ensure complete
 141 decarbonation of the samples. Early attempts involved subjecting the samples to gentle vacuum
 142 using a rotary evaporator, as successfully demonstrated by Blyth et al. (2013a), but this was
 143 quickly abandoned due to substantial blank contributions encountered with this method in our
 144 laboratory (Suppl. fig. 1). More efficient and less detrimental methods in terms of blank
 145 contributions were (i) to place the samples in a desiccator that was evacuated using a hand-held
 146 pump for a few days while periodically renewing the vacuum, or (ii) to subject the closed
 147 sample vials to sonication by placing them in an ultrasonic bath at room temperature for 30-45
 148 min during acidification.
 149



150
 151 **Fig. 2.:** Flowchart describing the method. The method steps covered by WCO and chemical
 152 pre-treatment (CPT) standards for blank assessment are indicated.

153

154 **Wet Chemical Oxidation and Isotope Analysis**

155 After decarbonation, organic carbon was converted to CO₂ using a wet chemical oxidation
 156 (WCO) approach (described in Lang et al., 2016, 2013, 2012, Fig. 2). Briefly, sodium persulfate

157 (Sigma, purum p.a. $\geq 99.0\%$, further purified by recrystallization) was added as an oxidant (1
158 ml; solution: 1.5g $\text{Na}_2\text{S}_2\text{O}_8$ in 50 ml ultrapure water) after the decarbonation. All vials were
159 capped and purged for ~ 10 min using ultrapure helium to remove ambient air and remaining
160 inorganic CO_2 in the vials. For the oxidation to take place, the vials were then heated to $\sim 100^\circ\text{C}$
161 for one hour (Fig. 2). The headspace CO_2 resulting from oxidation of the NPOC was analysed
162 for $\delta^{13}\text{C}$ on a Thermo Delta V Plus isotope ratio mass spectrometer (IRMS) coupled with a
163 ThermoFinnigan GasBench II carbonate preparation device at the Geological Institute, ETH
164 Zurich, following the method described in Lang et al. (2012). $\delta^{13}\text{C}$ values are reported as $^{13}\text{C}/^{12}\text{C}$
165 ratios expressed as the permil deviation from the international Vienna Pee Dee Belemnite
166 standard (VPDB). ^{14}C measurements were performed as described in Lang et al. (2016) using
167 a MICADAS AMS equipped with a Gas Ion Source (GIS) at the Laboratory for Ion Beam
168 Physics (LIP) at ETH Zurich. AMS background correction and data normalization were carried
169 out using the software BATS (Wacker et al., 2010) and $^{14}\text{C}/^{12}\text{C}$ ratios are reported as $F^{14}\text{C}$
170 according to (Reimer et al., 2004).

171

172 **Blank Assessment**

173 Sucrose (Sigma, $\delta^{13}\text{C} = -12.4\text{‰}$ VPDB, $F^{14}\text{C} = 1.053 \pm 0.003$) and phthalic acid (Sigma, $\delta^{13}\text{C}$
174 $= -33.6\text{‰}$ VPDB, $F^{14}\text{C} < 0.0025$) were used as standards to evaluate blank contributions from
175 the different steps of the method. These standards were chosen for their distinct isotope
176 signatures, which allow to capture different contamination end members, and their solubility in
177 water (Lang et al., 2016).

178 The contribution of extraneous carbon to the WCO was evaluated by a suite of standards (*WCO*
179 *standards*) prepared for each run by adding varying amounts of standard solution to vials
180 containing 5 ml of ultrapure water, then taking them through the WCO procedure. To evaluate
181 the mass and $F^{14}\text{C}$ of extraneous carbon for each run, we used the model of constant
182 contamination described in Hanke et al. (2017) and Haghypour et al. (2018). The procedural
183 blank of the decarbonation (*chemical pre-treatment standard*) was quantified by spiking vials
184 containing acid with variable amounts of sucrose and phthalic acid, before taking them through
185 the entire procedure (Fig. 2). The decarbonation efficiency and possible carbonate matrix
186 effects were tested by analysing carbonate samples with no oxidant added, and/or by spiking
187 IAEA-C1 (carbonate $F^{14}\text{C} = 0$, NPOC presumed ^{14}C -dead) samples with known amounts of
188 standard solution. Finally, we tested whether contamination from the rubber septa might pose
189 an issue with prolonged storage times of prepared extracts (three weeks). This was achieved by
190 preparing chemical pre-treatment standards that were subsequently measured in two batches,
191 the first one day and the second three weeks after preparation.

192

193 **RESULTS**

194 **Blank Assessment**

195 Because of the typically low amount of extraneous carbon in WCO samples, standard curves
 196 were used to assess blank contamination in each run. Using two standards with very different
 197 $F^{14}C$ and $\delta^{13}C$ values allows quantification of the amount and isotopic composition of the blank
 198 (Hanke et al., 2017; Lang et al., 2016). All runs were corrected for extraneous carbon
 199 contributions following the methodology by Hanke et al. (2017) for $F^{14}C$ and Lang et al. (2012)
 200 for $\delta^{13}C$ (not discussed here). Both methods assume constant contamination from each method
 201 step on all samples.

202

203 **Long-Term ^{14}C Blank Assessment of WCO Procedure**

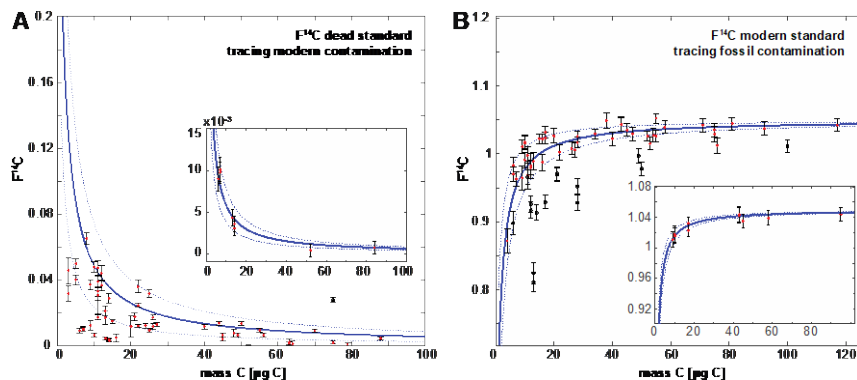
204 For the WCO standards (Fig. 3, Table 2), the average blank contamination over all runs was
 205 $1.30 \pm 0.52 \mu\text{g C}$, $F^{14}C = 0.42 \pm 0.17$, when calculated with the method of constant
 206 contamination by Haghypour et al. (2018; Suppl. Table 1). However, the fluctuation in the
 207 contribution of extraneous carbon varied greatly between runs over the course of the study
 208 (2015 – 2018). Within a single run, contamination can be as low as $0.4 \pm 0.1 \mu\text{g C}$ ($F^{14}C = 0.15$
 209 ± 0.04 , run C170918NHG1). For six out of the nine runs, contamination remained below 1.15
 210 $\mu\text{g C}$ and only two runs had contamination $> 3 \mu\text{g C}$ (Table 2).

211

Run number	WCO standards				Chemical pre-treatment standards				% blank from WCO
	$F^{14}C$	$\sigma_{F^{14}C}$ (abs)	mc (μg)	σ_{mc} (abs)	$F^{14}C$	$\sigma_{F^{14}C}$ (abs)	mc (μg)	σ_{mc} (abs)	
C180108NHG1	0.21	0.04	1.1	0.2	0.17	0.03	1.7	0.3	65
C170918NHG1	0.15	0.10	0.4	0.1	0.40	0.08	2.5	0.5	32
C160913FLG1	0.32	0.06	1.1	0.2	0.25	0.05	4.0	0.8	27
C160825BLVG1	0.47	0.09	0.9	0.2	0.30	0.06	4.3	0.9	22
C160510TVG1	0.17	0.03	1.8	0.4					
C160224FLG1	0.26	0.05	1.1	0.2					
C150903FLG1	0.11	0.02	3.1	0.6					
C150928FLG1	0.39	0.08	1.1	0.2					
C150602FLG1	0.09	0.02	3.3	0.7					

212 **Table 2.:** Blank contamination for all AMS runs for WCO standards, as well as the chemical
 213 pre-treatment standards (where available).

214



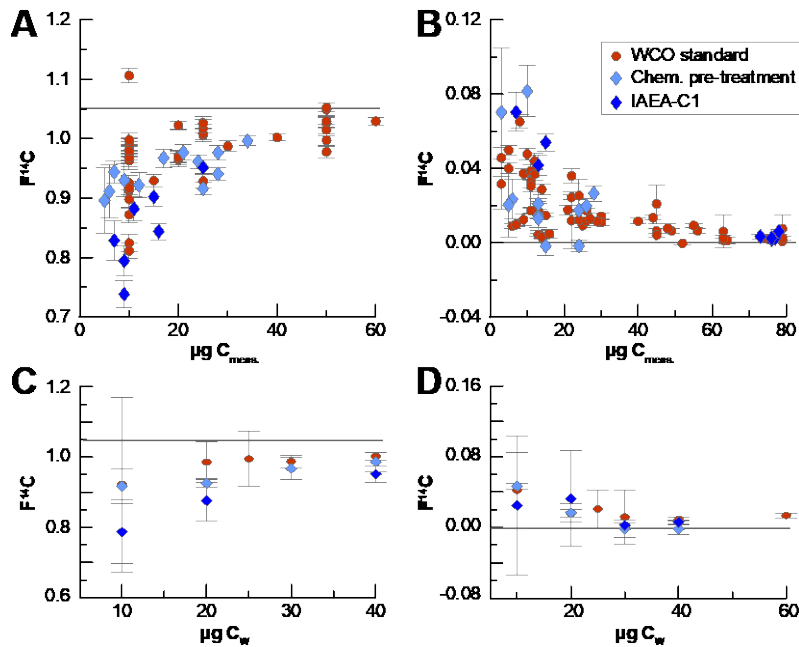
215
 216 **Fig. 3:** Summary of all WCO standards analysed in the course of the study. A – $F^{14}C$ of the
 217 dead standard, phthalic acid. B – $F^{14}C$ of the modern standard, sucrose. Outliers are marked in
 218 black and were not included in the calculation of the blank contribution. Inserts show values
 219 for a single measurement run. The solid blue lines represent the best fit with 1σ error ranges.
 220 All data is provided in Suppl. Table 1.

221

222 **Chemical Pre-Treatment Blank**

223 Overall, the chemical pre-treatment standards show larger blank contamination than the WCO
 224 ($1.7 \pm 0.34 - 4.3 \pm 0.86 \mu\text{g C}$, Table 2, Fig. 4), with the WCO contributing between 22 and 65%
 225 (average 37%, $n=4$) of the total extraneous carbon in the samples. The $F^{14}C$ values between
 226 individual chemical pre-treatment and WCO standards were usually within the 2σ -bound of
 227 each other, although contamination $F^{14}C$ values were always lower for the chemical pre-
 228 treatment standards. Incomplete removal of inorganic CO_2 from the sample solution proved to
 229 be one of the main challenges faced during method development. Tests on samples that were
 230 not oxidised and processed using the desiccator revealed that 23 out of 42 test vials contained
 231 small amounts of residual inorganic carbonate, with enriched $\delta^{13}\text{C}_{\text{CO}_2}$ values (average over all
 232 samples -8.92‰ VPDB). Sonication at room temperature also typically resulted in small (~ 0.7 -
 233 $1.5 \mu\text{g C}$) amounts of carbonate left in the solution. Vials containing known amounts of ^{14}C -
 234 dead IAEA-C1 carbonate and spiked with phthalic acid show a weak correlation between the
 235 amount of carbonate added and the isotopic composition of the WCO extract (Suppl. fig. 2),
 236 suggesting a possible influence of sample size on decarbonation efficiency. Rubber septa
 237 contamination during extract storage does not appear to be an issue over the timescale
 238 investigated here (up to three weeks). We find no significant difference between the average
 239 value of sucrose and phthalic acid samples measured before and after storage (sucrose values
 240 are within 1σ of each other, phthalic acid within 2σ , after blank correction).

241



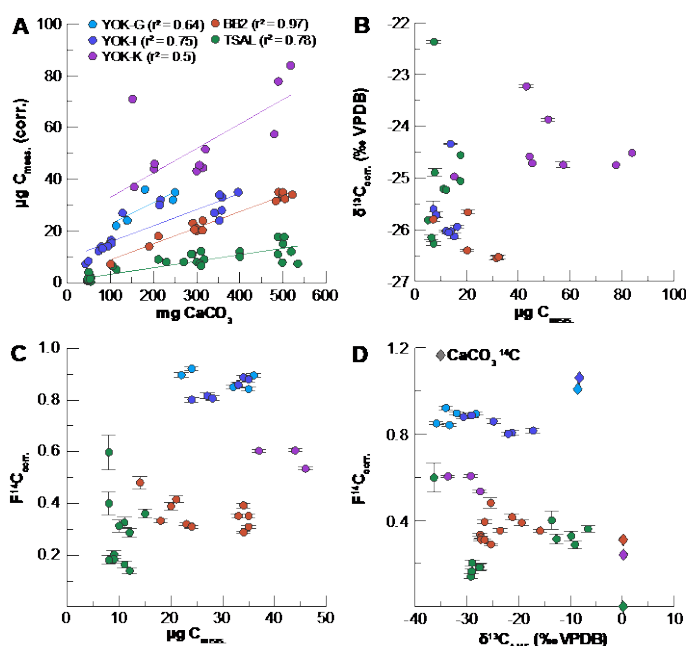
242
 243 **Fig. 4.:** Comparison between chemical pre-treatment and WCO standards, as well as IAEA-
 244 C1-spiked procedural standards, presumed NPOC-dead. A and B - standard curves for sucrose
 245 and phthalic acid, respectively, C and D – average of the standard groups per weight class
 246 (grouped by amount of standard weighed in).

247

248 **Stalagmites**

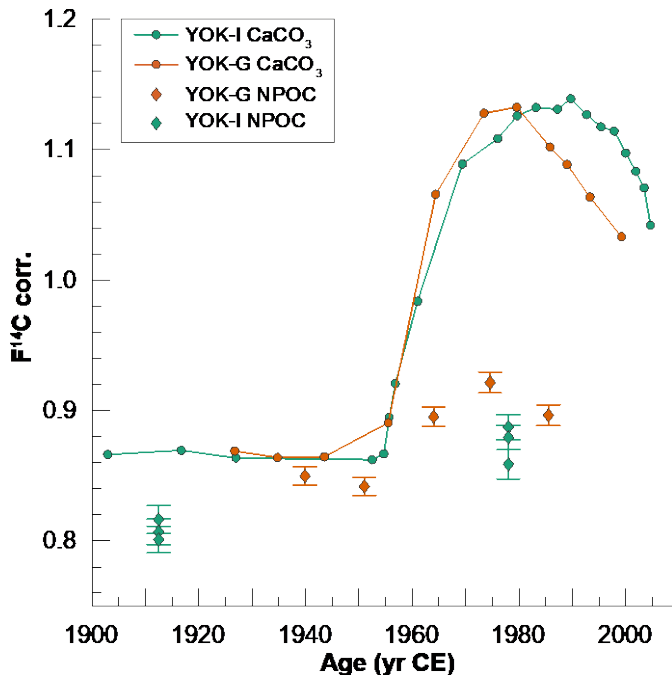
249 For each stalagmite, the amount of C measured is positively correlated to the initial carbonate
 250 sample size, and is fairly reproducible for different initial weights (Fig. 5A, Suppl. Table 2).
 251 NPOC concentrations vary greatly between stalagmites, ranging between 0.003 and 0.017 wt%
 252 (averages calculated for all samples of one stalagmite), with TSAL yielding the lowest
 253 concentrations and YOK-G and YOK-K the highest. These NPOC concentrations are within
 254 the range of previously published values for speleothems (0.01 – 0.3 wt%, Blyth et al., 2016;
 255 Li et al., 2014; Quiers et al., 2015). Most stalagmite WCO extracts are depleted in ^{13}C , with
 256 $\delta^{13}\text{C}$ values clustering around -24 – -26‰ VPDB, values typical of C3 vegetation (Fig.
 257 7B). No clear trend in $\delta^{13}\text{C}$ values between the different stalagmites can be discerned, and the
 258 intra-sample variability in $\delta^{13}\text{C}$ is generally larger than the difference between samples.
 259 $F^{14}\text{C}$ values show no trend with sample size, and appear to be relatively consistent for the
 260 different stalagmites (Fig. 5C, Suppl. Table 2). TSAL, the oldest stalagmite (40 kyr) also
 261 exhibits the lowest NPOC ^{14}C activities (average $F^{14}\text{C} = 0.29$), but these values are still
 262 significantly higher than the corresponding carbonate value ($F^{14}\text{C} \sim 0$, Fig. 5D). Stalagmite

263 YOK-K (estimated age ~2 kyr) shows the same trend (NPOC $F^{14}C = 0.52$, $CaCO_3 F^{14}C = 0.24$),
 264 whereas no difference is found between NPOC and $CaCO_3$ in stalagmite BB2 (assumed age: 3-
 265 6 kyr, NPOC $F^{14}C = 0.35$, $CaCO_3 F^{14}C = 0.31$). For YOK-I and YOK-G (covering the bomb
 266 spike interval), the trend is reversed, with the $CaCO_3 F^{14}C$ higher than the NPOC $F^{14}C$ (YOK-
 267 I: NPOC $F^{14}C = 0.77$, $CaCO_3 F^{14}C = 1.0$; YOK-G: NPOC $F^{14}C = 0.88$, $CaCO_3 F^{14}C = 1.01$).
 268



269
 270 **Fig. 5.:** Results of the stalagmite samples. A – Amount of carbon ($\mu g C$) measured and corrected
 271 for procedural blanks vs. weight of $CaCO_3$ (in mg) added to the vials for all stalagmites used
 272 in this study. Data is combined from all runs for $\delta^{13}C$ and ^{14}C . B – Blank corrected $\delta^{13}C$ values
 273 from IRMS vs. amount of C measured. C – $F^{14}C$ vs. amount of C measured. D – $F^{14}C$ vs. $\delta^{13}C$
 274 from the same AMS run. Note that the precision on AMS $\delta^{13}C$ is $\pm 2\%$. Diamonds denote the
 275 corresponding values measured on carbonate samples.
 276

277 The pre- and post-bomb spike NPOC samples from stalagmites YOK-I and YOK-G both show
 278 an increase in $F^{14}C$ with the bomb spike (Fig. 6). However, in both cases, the NPOC $F^{14}C$ is
 279 lower than the contemporaneous carbonate $F^{14}C$. Samples from the first batch of samples from
 280 YOK-I (YOK-I A, analysed in May 2016) have markedly lower $F^{14}C$ and less negative $\delta^{13}C$
 281 values compared to both a previous analysis and to the samples of YOK-G (Suppl. Fig. 4).
 282



283
 284 **Fig. 6.:** Comparison between the bomb spike measured in stalagmites YOK-I and YOK-G
 285 carbonate with the results from WCO measurements on NPOC extracts.

286
 287 **DISCUSSION**

288 **Method Evaluation**

289 The method described here holds promise as a fast and simple procedure to extract and isolate
 290 NPOC from carbonate samples. Extensive testing has provided encouraging results, which
 291 provide a foundation for further development and refinement of the method. One of the key
 292 advantages of the method lies in the comparatively small sample sizes required. Depending on
 293 the amount of NPOC present in a stalagmite, as little as 50 mg sample mass are required for a
 294 high-precision IRMS $\delta^{13}\text{C}$ measurement, and 100-200 mg for an AMS ^{14}C measurement. This
 295 is similar to amounts reported by Blyth et al. (2013a, 2013b) for $\delta^{13}\text{C}$, and paves the way for
 296 conducting high-resolution studies of isotopic variations in NPOC from stalagmites.
 297 Additionally, the simple procedure, conducted entirely in one single vial, greatly reduces the
 298 risk of contamination by laboratory procedures, considered a major problem for studies of
 299 organic matter in stalagmites (Wynn and Brocks, 2014). Indeed, the contamination on single
 300 runs with this method can be as low as $0.4 \pm 0.1 \mu\text{g C}$ ($F^{14}\text{C}$ 0.15 ± 0.04), which greatly improves
 301 confidence in the interpretation of NPOC $\delta^{13}\text{C}$ and ^{14}C signatures even on very small samples
 302 ($<10 \mu\text{g C}$). Due to blank fluctuations, we recommend running a complete standard curve,

303 ideally with 5 or more standards for both end members, with each sample run. Moreover, it
304 appears that the sucrose standard is very susceptible to degradation once in solution, and future
305 tests should investigate the use of a different modern standard with similar specifications (e.g.,
306 oxalic acid). Lowest blank contributions are typically obtained using freshly prepared standard
307 solutions and oxidant (re-precipitated using ultra-pure water). The chemical pre-treatment
308 standards tend to have slightly lower $F^{14}C$ compared to the WCO standards (but the difference
309 is not significant), which could point towards a minor blank contribution from the H_3PO_4 .
310 Although previous studies did not report blank issues related to the acid used (Lang et al., 2016,
311 2013, 2012), future studies should investigate how the much larger volume of acid needed for
312 this method might influence overall blank contributions (e.g., Blyth et al., 2006). Storage times
313 of up to three weeks do not result in increased blank contribution, e.g., from rubber septa
314 degradation. However, we still recommend swift analysis of prepared extracts, ideally within
315 days of the oxidation (but allowing enough time for solution re-equilibration after sample
316 heating, i.e., ~24 hours), to achieve best results. Finally, prolonged storage of powdered
317 carbonate samples should be avoided, as sorption of extraneous carbon on carbonate is common
318 (Stipp and Hochella, 1991). Both stalagmites YOK-I and YOK-G were sampled shortly (hours
319 – days) before analysis, and therefore we do not expect sorption effects to play a major role.
320 Confidence in the results presented here stem from (i) steadily increasing NPOC concentrations
321 with increasing sample size, suggesting that the carbon extracted is likely inherent to the
322 sample, and not introduced by external background contamination, and (ii) NPOC $\delta^{13}C$ values
323 that are consistent with organic biomass, most likely reflecting carbon sources from terrestrial
324 vegetation or microbial activity. However, our results show significant variability, both within
325 replicate NPOC samples, as well as in the relationship between NPOC and $CaCO_3$ values. This
326 is likely the result of variable matrix effects as a function of sample type, as well in some cases
327 incomplete decarbonation. We discuss these issues further below.

328

329 **Decarbonation Efficiency**

330 Ensuring the complete removal of inorganic carbon proved to be the most difficult step of the
331 method development. Subjecting the samples to a weak vacuum or to sonication was often
332 successful in removing all $CaCO_3$ from the solution, but the efficacy of the method still has
333 reproducibility issues, especially for some stalagmites (e.g., TSAL). Decarbonation using
334 rotary evaporation was the only method that reliably removed all $CaCO_3$ from solution in all
335 tested stalagmites, but in our case introduced large blanks, probably from the oil pumps (Suppl.
336 fig. 1). However, this should not discourage others to test the use of a rotary evaporator, as this
337 is the standard technique for DOC analysis of aquatic samples, and can often be employed
338 successfully (Bryan et al., 2017). The other methods tested (desiccator and sonication) have the
339 advantage of allowing a much higher throughput of sample batches compared to the rotary

Commented [SSE3]: Okay, but didn't some of your previous results suggest that this isn't much of an issue in reality?

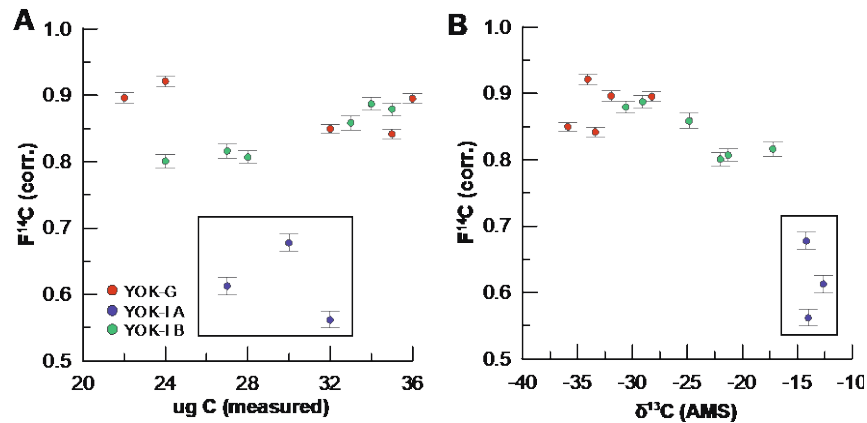
340 evaporator, an essential quality if the method is to be applied to high-resolution studies. In this
341 study, reproducibility and decarbonation efficiency were assessed by analysing chemical pre-
342 treatment standards and carbonate samples without oxidant. This approach, albeit time and
343 resource consuming, allows to assess contamination and decarbonation individually, ideally for
344 each run, and is advantageous for cases where method reproducibility is problematic.

345 Quantification of the amount of inorganic carbon in the NPOC extracts remains difficult,
346 because the amount and isotope value of the organic 'end member' is not known. A simple
347 isotopic mass balance can be carried out:

$$348 \quad A_m \times \delta^{13}C_m = X \times \delta^{13}C_{ic} + (A_m - X) \times \delta^{13}C_{oc} \quad (1)$$

349 where A_m and $\delta^{13}C_m$ are the measured amount and $\delta^{13}C$ of carbon in the samples, $\delta^{13}C_{ic}$ is the
350 $\delta^{13}C$ of the inorganic carbon, $\delta^{13}C_{oc}$ is the $\delta^{13}C$ value of the organic end member. X is the
351 amount of inorganic carbon. We assume that the OC is entirely derived from C3-plants, a good
352 approximation for all the caves studied here, resulting in an organic end member $\delta^{13}C$ value of
353 -25‰ VPDB. For stalagmite YOK-K, which shows the most consistent $\delta^{13}C$ values for NPOC
354 (Fig. 5B), mass balance reveals that about 1.2 - 4 μg C are likely CaCO_3 -derived, which
355 amounts to 2-11% of the original CaCO_3 remaining in the solution. For the other stalagmites,
356 the scatter between different measurements is much larger, and it is not straightforward to
357 calculate the amount of CaCO_3 remaining in the solution. This shows that complete removal of
358 residual inorganic carbon from the samples remains a challenge, with implications for the
359 fidelity of isotopic values measured in NPOC. Residual carbonate can also be detected in the
360 IAEA-C1 vials spiked with phthalic acid (Suppl. Fig. 2), where larger samples display lower
361 $F^{14}C$ and less negative $\delta^{13}C$ values, suggesting incomplete decarbonation. This was confirmed
362 by tests using the IAEA-C2 standard ($F^{14}C = 0.41$, $\delta^{13}C = -8.25\text{‰}$ VPDB, not shown).

363 Combined $\delta^{13}C$ and ^{14}C datasets can help distinguish and exclude compromised samples. For
364 example, samples from YOK-I batch A (YOK-I A, analysed in May 2016) have markedly lower
365 $F^{14}C$ and less negative $\delta^{13}C$ values compared to both a previous analysis and to the samples of
366 YOK-G (Fig. 7). These results suggest that the YOK-I A samples are affected by incomplete
367 decarbonation, and thus should be excluded from further interpretation. Similarly, TSAL
368 proved to be an especially difficult stalagmite to achieve complete decarbonation, which might
369 point towards an inherent matrix effect that is more pronounced in this stalagmite than in others
370 (Suppl. Fig. 3). More detailed studies of mineralogy and microstructure (e.g., through X-ray
371 diffraction or scanning electron microscopy) in the samples should be encouraged in future
372 studies, to better characterise the sample matrix.



373
 374 **Fig. 7.:** Comparison of the results for stalagmites YOK-I and YOK-G. Samples from YOK-I
 375 analysed during May 2016 (YOK-I A), likely affected by incomplete decarbonation, are
 376 highlighted by the black box.

377

378 **Significance for interpretation of NPOC in stalagmites**

379 The pronounced bomb spikes found in the carbonate of stalagmites YOK-I and YOK-G (Fig.
 380 6) suggests that the majority of carbon transferred to the cave is cycled rapidly, and no large
 381 reservoir of pre-aged carbon is present. Previously published results on ^{14}C analysis of water
 382 extractable organic carbon (WEOC) from soil samples collected above the Yok Balum Cave
 383 reflect the dominant contribution of very young OC from the soil, with 96% of the soil carbon
 384 being less than 50 years old (Lechleitner et al., 2016b). This is likely a function of the shallow
 385 thickness of the host rock above the cave (~ 14 m), and the rapid response of the active drips
 386 to increases in rainfall (peaks during large rainfall events, and a general increase in drip rate
 387 over the rainy season; Ridley et al., 2015), which lead to rapid surface to cave signal transfer
 388 and minimise input from deeper carbon sources within the host rock. Compared to the test
 389 stalagmites from mid-latitude sites (BB2 and TSAL), the Yok Balum Cave stalagmites have
 390 higher concentrations of NPOC, which might additionally point towards a faster carbon transfer
 391 at this tropical location (Fig. 5A).

392 The NPOC $F^{14}C$ from stalagmites YOK-I and YOK-G shows good agreement with the
 393 progression of the bomb spike rise in the carbonate of both stalagmites (Fig. 6). Compared to
 394 the carbonate $F^{14}C$ however, the NPOC signal is dampened and overall $F^{14}C$ is much lower.
 395 This is somewhat counterintuitive, as one would expect the carbonate, affected by ^{14}C -dead
 396 host rock carbon, to be more depleted with respect to the vegetation-derived NPOC $F^{14}C$. At
 397 this stage, methodological issues, such as an unaccounted contamination source or stripping of
 398 more volatile molecules during purging (Lang et al., 2016, 2010) cannot be entirely ruled out.
 399 However, our extensive blank assessment, and the fact that the chemical pre-treatment

400 standards are not significantly different from the WCO standards, suggest that our results are
401 robust, and the signal is likely real. One way to explain the difference between NPOC and
402 carbonate ^{14}C signatures in stalagmites YOK-I and YOK-G is through a contribution of OC
403 from a refractory (insoluble and non-hydrolysable) pool that is not sourced from the soil. This
404 could be related to a deep carbon source in the karst, as previously recognised in other karst
405 systems (Benavente et al., 2010; Bergel et al., 2017; Matthey et al., 2016; Noronha et al., 2015).
406 Although these studies focused on the presence of elevated $p\text{CO}_2$ deeper in the karst that
407 contribute carbon depleted in ^{14}C to the drip water solution, it is also possible that refractory
408 organic compounds are transported to the cave from such a source. Similarly, organic matter
409 produced *in situ* (on the cave walls or on the stalagmites themselves) by microbial communities
410 has been suggested as an important source of OC in stalagmites (Blyth et al., 2014; Lechleitner
411 et al., 2017; Tisato et al., 2015), and could be responsible for the divergence between inorganic
412 and organic carbon in stalagmites. A third potential source of refractory carbon in the karst
413 system is fossil OC leached from the bedrock carbonate rock itself, e.g., through partial
414 microbial oxidation. Such 'petrogenic OC' can have a measurable impact on bulk F^{14}C values,
415 e.g., in rivers (Bouchez et al., 2010; Galy et al., 2008; Hemingway et al., 2018), and has been
416 identified as an important component of speleothem OC before (Gázquez et al., 2012). One
417 challenge to these explanations is the inverse trend found in stalagmite YOK-K, where the
418 carbonate ^{14}C is older than the NPOC, which might point towards contamination from a modern
419 OC source during sampling, given that this is the sample with the highest NPOC concentrations
420 tested here.

421 At present, our dataset does not allow a more definitive attribution of a single process (or a
422 combination of several processes) that can explain the contrasting behaviour of inorganic and
423 organic carbon in the stalagmites. It should be noted, however, that a previous study seeking to
424 characterise the molecular spectrum of the dissolved organic matter (DOM) at Yok Balum Cave
425 found very different molecular composition of soil and drip waters, and stalagmites, with the
426 stalagmite DOM fingerprint suggesting a contribution from microbial organic matter
427 (Lechleitner et al., 2017). Irrespective of these unresolved issues, it is clear that at Yok Balum
428 Cave, OC entrapped within stalagmites derives from one or several dynamic pool(s). Whether
429 stalagmites from other locations (e.g., high latitudes) exhibit similar characteristics, both in the
430 magnitude and cycling of organic matter, remains to be seen.

431

432 CONCLUSIONS

433 We present first results from a method development study on extraction and isotopic ($\delta^{13}\text{C}$ and
434 ^{14}C) characterisation of speleothem NPOC. The advantages of the method lie in its simple, rapid
435 protocol that is carried out in a single vial, minimising the potential for contamination through
436 laboratory procedures, and in the small sample sizes needed. Encouraging results indicate that

437 the extracted carbon is likely inherent to the sample and organic, as shown by depleted $\delta^{13}\text{C}$
438 values. However, unresolved issues remain, and need to be addressed by future studies to fully
439 make use of the method. A major remaining issue is incomplete sample decarbonation, resulting
440 in biased isotope values. Although anomalous samples can be detected via combined $\delta^{13}\text{C}$ and
441 ^{14}C analyses, further methodological improvements are needed before the method can be made
442 routine. Complete decarbonation was so far achieved only when subjecting the samples to a
443 weak vacuum using a rotary evaporator. Unfortunately, this method had to be abandoned as it
444 resulted in contamination of the samples from the oil pump. Sonication appears to be a
445 promising tool to increase decarbonation efficiency, with the advantage of working on a closed
446 vial and thus minimising contamination, but needs to be tested more thoroughly. Sample
447 contamination through laboratory procedures need to be minimised, as this method is very
448 susceptible to blank effects. Ideally, a designated “clean” fume hood should be used for this
449 method only, and in any case work producing large amounts of dust should not be carried out
450 in the same room as the wet oxidation procedure. The sucrose standard appears to be very
451 susceptible to alteration, and might be better replaced by another compound with modern F^{14}C
452 and similar $\delta^{13}\text{C}$ (e.g., oxalic acid).

453 Subsequent studies that further improve upon methodologies and expand measurements to a
454 broader suite of stalagmites and their host cave systems should add important new constraints
455 on carbon cycle processes in karst systems and organic signals preserved in stalagmites.
456 Moreover, detailed investigations on organic and inorganic carbon fluxes in karst systems and
457 the isotopic fingerprint of processes acting on them could provide important insights into the
458 local carbon cycle and the sources of carbon in speleothems.

459

460 **ACKNOWLEDGEMENT**

461 We thank the staff at LIP, especially Lukas Wacker, and Daniel Montluçon, Stewart Bishop
462 and Madalina Jaggi at the Geological Institute, ETH Zurich for their assistance with sample
463 analysis. We thank José Mes for assistance during fieldwork at Yok Balum Cave. We gratefully
464 acknowledge Sebastian Breitenbach, Denis Scholz, and Birgit Plessen for provision of sample
465 materials from stalagmites BB2 and TSAL. We thank Andy Baker and Kathleen Johnson for
466 critical reviewing of this manuscript, and the editorial team at *Radiocarbon*. This research was
467 supported by the European Research Council grant 240167 grant to JULB, and by Swiss
468 National Science Foundation grant P2EZP2_172213 to FAL. Field collection was supported
469 additionally by the National Science Foundation (grant HSD 0827305) and the Alphawood
470 Foundation.

471

472 **REFERENCES**

473 Baker, A., Genty, D., 1999. Fluorescence wavelength and intensity variations of cave waters.

474 J. Hydrol. 217, 19–34. doi:10.1016/S0022-1694(99)00010-4

475 Benavente, J., Vadillo, I., Carrasco, F., Soler, A., Liñán, C., Moral, F., 2010. Air Carbon
476 Dioxide Contents in the Vadose Zone of a Mediterranean Karst. *Vadose Zo. J.* 9, 126–
477 136. doi:10.2136/vzj2009.0027

478 Bergel, S.J., Carlson, P.E., Larson, T.E., Wood, C.T., Johnson, K.R., Banner, J.L., Breecker,
479 D.O., 2017. Constraining the subsoil carbon source to cave-air CO₂ and speleothem
480 calcite in central Texas. *Geochim. Cosmochim. Acta* 217, 112–127.
481 doi:10.1016/j.gca.2017.08.017

482 Birdwell, J.E., Engel, A.S., 2010. Characterization of dissolved organic matter in cave and
483 spring waters using UV-Vis absorbance and fluorescence spectroscopy. *Org. Geochem.*
484 41, 270–280. doi:10.1016/j.orggeochem.2009.11.002

485 Blyth, A.J., Baker, A., Collins, M.J., Penkman, K.E.H., Gilmour, M.A., Moss, J.S., Genty, D.,
486 Drysdale, R.N., 2008. Molecular organic matter in speleothems and its potential as an
487 environmental proxy. *Quat. Sci. Rev.* 27, 905–921. doi:10.1016/j.quascirev.2008.02.002

488 Blyth, A.J., Farrimond, P., Jones, M., 2006. An optimised method for the extraction and
489 analysis of lipid biomarkers from stalagmites. *Org. Geochem.* 37, 882–890.
490 doi:10.1016/j.orggeochem.2006.05.003

491 Blyth, A.J., Hartland, A., Baker, A., 2016. Organic proxies in speleothems - New
492 developments, advantages and limitations. *Quat. Sci. Rev.* 149, 1–17.
493 doi:10.1016/j.quascirev.2016.07.001

494 Blyth, A.J., Hua, Q., Smith, A., Frisia, S., Borsato, A., Hellstrom, J., 2017. Exploring the
495 dating of “dirty” speleothems and cave sinters using radiocarbon dating of preserved
496 organic matter. *Quat. Geochronol.* 39, 92–98. doi:10.1016/j.quageo.2017.02.002

497 Blyth, A.J., Jex, C.N., Baker, A., Khan, S.J., Schouten, S., 2014. Contrasting distributions of
498 glycerol dialkyl glycerol tetraethers (GDGTs) in speleothems and associated soils. *Org.*
499 *Geochem.* 69, 1–10. doi:10.1016/j.orggeochem.2014.01.013

500 Blyth, A.J., Shutova, Y., Smith, C., 2013a. $\delta^{13}\text{C}$ analysis of bulk organic matter in
501 speleothems using liquid chromatography-isotope ratio mass spectrometry. *Org.*
502 *Geochem.* 55, 22–25. doi:10.1016/j.orggeochem.2012.11.003

503 Blyth, A.J., Smith, C.I., Drysdale, R.N., 2013b. A new perspective on the $\delta^{13}\text{C}$ signal
504 preserved in speleothems using LC-IRMS analysis of bulk organic matter and
505 compound specific stable isotope analysis. *Quat. Sci. Rev.* 75, 143–149.
506 doi:10.1016/j.quascirev.2013.06.017

507 Borsato, A., Frisia, S., Jones, B., van der Borg, K., 2000. Calcite moonmilk: crystal
508 morphology and environment of formation in caves in the Italian Alps. *J. Sediment. Res.*
509 70, 1170–1190.

510 Bosle, J.M., Mischel, S.A., Schulze, A.-L., Scholz, D., Hoffmann, T., 2014. Quantification of

511 low molecular weight fatty acids in cave drip water and speleothems using HPLC-ESI-
512 IT / MS — development and validation of a selective method. *Anal. Bioanal. Chem.*
513 406, 3167–3177. doi:10.1007/s00216-014-7743-6

514 Bouchez, J., Beyssac, O., Galy, V., Gaillardet, J., France-Lanord, C., Maurice, L., Moreira-
515 Turcq, P., 2010. Oxidation of petrogenic organic carbon in the Amazon floodplain as a
516 source of atmospheric CO₂. *Geology* 38, 255–258. doi:10.1130/G30608.1

517 Bryan, E., Meredith, K.T., Baker, A., Andersen, M.S., Post, V.E.A., 2017. Carbon dynamics
518 in a Late Quaternary-age coastal limestone aquifer system undergoing saltwater
519 intrusion. *Sci. Total Environ.* 607–608, 771–785. doi:10.1016/j.scitotenv.2017.06.094

520 Einsiedl, F., Hertkorn, N., Wolf, M., Frommberger, M., Schmitt-Kopplin, P., Koch, B.P.,
521 2007. Rapid biotic molecular transformation of fulvic acids in a karst aquifer. *Geochim.*
522 *Cosmochim. Acta* 71, 5474–5482. doi:10.1016/j.gca.2007.09.024

523 Fahrni, S.M., Wacker, L., Synal, H.A., Szidat, S., 2013. Improving a gas ion source for 14C
524 AMS. *Nucl. Instruments Methods Phys. Res. Sect. B* 294, 320–327.
525 doi:10.1016/j.nimb.2012.03.037

526 Galy, V., Beyssac, O., France-Lanord, C., Eglinton, T., 2008. Recycling of graphite during
527 Himalayan erosion: A geological stabilization of carbon in the crust. *Science* (80-.).
528 322, 943–945. doi:10.1126/science.1161408

529 Gázquez, F., Calaforra, J.M., Rull, F., Forti, P., García-Casco, A., 2012. Organic matter of
530 fossil origin in the amberine speleothems from El Soplao Cave (Cantabria, Northern
531 Spain). *Int. J. Speleol.* 41, 113–123. doi:10.5038/1827-806X.41.1.12

532 Genty, D., Konik, S., Valladas, H., Blamart, D., Hellstrom, J., Touma, M., Moreau, C.,
533 Dumoulin, J.-P., Nouet, J., Dauphin, Y., Weil, R., 2011. Dating the lascaux cave gour
534 formation. *Radiocarbon* 53, 479–500.

535 Haghypour, N., Ausin, B., Usman, M., Ishikawa, N.F., Wacker, L., Welte, C., Ueda, K.,
536 Eglinton, T.I., 2018. Compound-Specific Radiocarbon Analysis (CSRA) by Elemental
537 Analyzer- Accelerator Mass Spectrometry (EA-AMS): Precision and Limitations. *Anal.*
538 *Chem.* doi:10.1021/acs.analchem.8b04491

539 Hanke, U.M., Wacker, L., Haghypour, N., Schmidt, M.W.I., Eglinton, T.I., McIntyre, C.P.,
540 2017. Comprehensive radiocarbon analysis of benzene polycarboxylic acids (BPCAs)
541 derived from pyrogenic carbon in environmental samples. *Radiocarbon* 59, 1103–1116.
542 doi:10.1017/RDC.2017.44

543 Heidke, I., Scholz, D., Hoffmann, T., 2018. Quantification of lignin oxidation products as
544 vegetation biomarkers in speleothems and cave drip water. *Biogeosciences* 15, 5831–
545 5845. doi:10.5194/bg-2018-253

546 Hemingway, J.D., Hilton, R.G., Hovius, N., Eglinton, T.I., Haghypour, N., Wacker, L., Chen,
547 M., Galy, V. V., 2018. Microbial oxidation of lithospheric organic carbon in rapidly

548 eroding tropical mountain soils. *Science* (80-.). 360, 209–212.
549 doi:10.1126/science.aao6463

550 Lang, S.Q., Bernasconi, S.M., Früh-Green, G.L., 2012. Stable isotope analysis of organic
551 carbon in small ($\mu\text{g C}$) samples and dissolved organic matter using a GasBench
552 preparation device. *Rapid Commun. Mass Spectrom.* 26, 9–16. doi:10.1002/rcm.5287

553 Lang, S.Q., Butterfield, D.A., Schulte, M., Kelley, D.S., Lilley, M.D., 2010. Elevated
554 concentrations of formate, acetate and dissolved organic carbon found at the Lost City
555 hydrothermal field. *Geochim. Cosmochim. Acta* 74, 941–952.
556 doi:10.1016/j.gca.2009.10.045

557 Lang, S.Q., Früh-Green, G.L., Bernasconi, S.M., Wacker, L., 2013. Isotopic (d^{13}C , D^{14}C)
558 analysis of organic acids in marine samples using wet chemical oxidation. *Limnol.*
559 *Oceanogr. Methods* 11, 161–175. doi:10.4319/lom.2013.11.161

560 Lang, S.Q., McIntyre, C.P., Bernasconi, S.M., Früh-Green, G.L., Voss, B.M., Eglinton, T.I.,
561 Wacker, L., 2016. Rapid ^{14}C Analysis of Dissolved Organic Carbon in Non-Saline
562 Waters. *Radiocarbon* 58, 505–515. doi:10.1017/RDC.2016.17

563 Lechleitner, F.A., Baldini, J.U.L., Breitenbach, S.F.M., Fohlmeister, J., McIntyre, C.,
564 Goswami, B., Jamieson, R.A., van der Voort, T.S., Prufer, K., Marwan, N., Culleton,
565 B.J., Kennett, D.J., Asmerom, Y., Polyak, V., Eglinton, T.I., 2016a. Hydrological and
566 climatological influences on a very high resolution tropical stalagmite radiocarbon
567 record. *Geochim. Cosmochim. Acta*. doi:http://dx.doi.org/10.1016/j.gca.2016.08.039

568 Lechleitner, F.A., Baldini, J.U.L., Breitenbach, S.F.M., Fohlmeister, J., McIntyre, C.,
569 Goswami, B., Jamieson, R.A., van der Voort, T.S., Prufer, K., Marwan, N., Culleton,
570 B.J., Kennett, D.J., Asmerom, Y., Polyak, V., Eglinton, T.I., 2016b. Hydrological and
571 climatological controls on radiocarbon concentrations in a tropical stalagmite. *Geochim.*
572 *Cosmochim. Acta* 194, 233–252. doi:10.1016/j.gca.2016.08.039

573 Lechleitner, F.A., Dittmar, T., Baldini, J.U.L., Prufer, K.M., Eglinton, T.I., 2017. Molecular
574 signatures of dissolved organic matter in a tropical karst system. *Org. Geochem.* 113.
575 doi:10.1016/j.orggeochem.2017.07.015

576 Li, X., Hu, C., Huang, J., Xie, S., Baker, A., 2014. A 9000-year carbon isotopic record of
577 acid-soluble organic matter in a stalagmite from Heshang Cave, central China:
578 Paleoclimate implications. *Chem. Geol.* 388, 71–77.
579 doi:10.1016/j.chemgeo.2014.08.029

580 Matthey, D.P., Atkinson, T.C., Barker, J.A., Fisher, R., Latin, J.-P., Durell, R., Ainsworth, M.,
581 2016. Carbon dioxide, ground air and carbon cycling in Gibraltar karst. *Geochim.*
582 *Cosmochim. Acta* 184, 88–113. doi:10.1016/j.gca.2016.01.041

583 Noronha, A.L., Johnson, K.R., Southon, J.R., Hu, C.C., Ruan, J., McCabe-Glynn, S., 2015.
584 Radiocarbon evidence for decomposition of aged organic matter in the vadose zone as

585 the main source of speleothem carbon. *Quat. Sci. Rev.* 127, 37–47.
586 doi:10.1016/j.quascirev.2015.05.021

587 Perrette, Y., Poulencard, J., Protière, M., Fanget, B., Lombard, C., Miège, C., Quiers, M.,
588 Nafferchoux, E., Pépin-Donat, B., 2015. Determining soil sources by organic matter
589 EPR fingerprints in two modern speleothems. *Org. Geochem.* 88, 59–68.
590 doi:10.1016/j.orggeochem.2015.08.005

591 Quiers, M., Perrette, Y., Chalmin, E., Fanget, B., Poulencard, J., 2015. Geochemical mapping
592 of organic carbon in stalagmites using liquid-phase and solid-phase fluorescence. *Chem.*
593 *Geol.* 411, 240–247. doi:10.1016/j.chemgeo.2015.07.012

594 Reimer, P.J., Brown, T.A., Reimer, R.W., 2004. Discussion: reporting and calibration of post-
595 bomb 14C data. *Radiocarbon* 46, 1299–1304.

596 Ridley, H.E., Asmerom, Y., Baldini, J.U.L., Breitenbach, S.F.M., Aquino, V. V., Pruffer,
597 K.M., Culleton, B.J., Polyak, V., Lechleitner, F.A., Kennett, D.J., Zhang, M., Marwan,
598 N., Macpherson, C.G., Baldini, L.M., Xiao, T., Peterkin, J.L., Awe, J., Haug, G.H.,
599 2015. Aerosol forcing of the position of the intertropical convergence zone since ad
600 1550. *Nat. Geosci.* 8, 195–200. doi:10.1038/ngeo2353

601 Ruff, M., Wacker, L., Gäggeler, H.W., Suter, M., Synal, H.-A., Szidat, S., 2007. A gas ion
602 source for radiocarbon measurements at 200 kV. *Radiocarbon* 49, 307–314.

603 Shabarova, T., Villiger, J., Morenkov, O., Niggemann, J., Dittmar, T., Pernthaler, J., 2014.
604 Bacterial community structure and dissolved organic matter in repeatedly flooded
605 subsurface karst water pools. *Microbiol. Ecol.* 89, 111–126. doi:10.1111/1574-
606 6941.12339

607 Stipp, S.L., Hochella, M.F.J., 1991. Structure and bonding environments at the calcite surface
608 as observed with X-ray photoelectron spectroscopy (XPS) and low energy electron
609 diffraction (LEED). *Geochim. Cosmochim. Acta* 55, 1723–1736.

610 Tisato, N., Torriani, S.F.F., Montoux, S., Sauro, F., De Waele, J., Tavagna, M.L., D'Angeli,
611 I.M., Chailloux, D., Renda, M., Eglinton, T.I., Bontognali, T.R.R., 2015. Microbial
612 mediation of complex subterranean mineral structures. *Sci. Rep.* 5, 15525.
613 doi:10.1038/srep15525

614 Vogel, J.C., 1980. Fractionation of the Carbon Isotopes During Photosynthesis, in:
615 *Sitzungsberichte Der Heidelberger Akademie Der Wissenschaften.* pp. 111–135.

616 Wacker, L., Christl, M., Synal, H.A., 2010. Bats: A new tool for AMS data reduction. *Nucl.*
617 *Instruments Methods Phys. Res. Sect. B* 268, 976–979. doi:10.1016/j.nimb.2009.10.078

618 Wynn, P.M., Brocks, J.J., 2014. A framework for the extraction and interpretation of organic
619 molecules in speleothem carbonate. *Rapid Commun. Mass Spectrom.* 28, 845–854.
620 doi:10.1002/rcm.6843

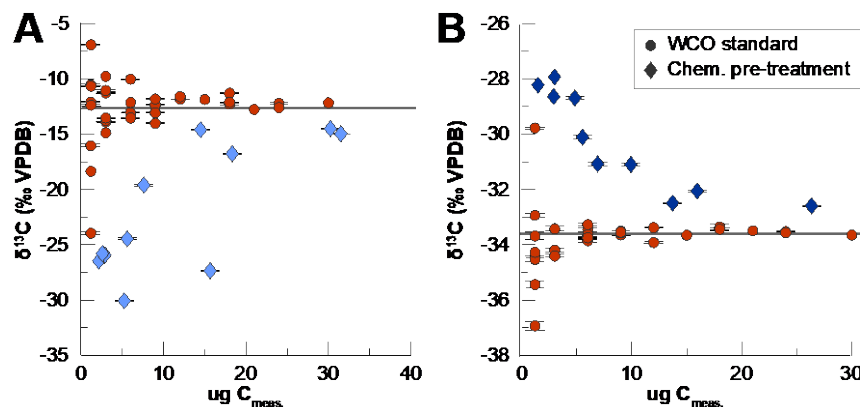
621

622 **Supplementary materials:**

623 **Supplementary Table 1:** Summary of all standards processed during this study, with their
624 blank correction according to Hanke et al. (2017) and Haghypour et al., (*in review*).

625

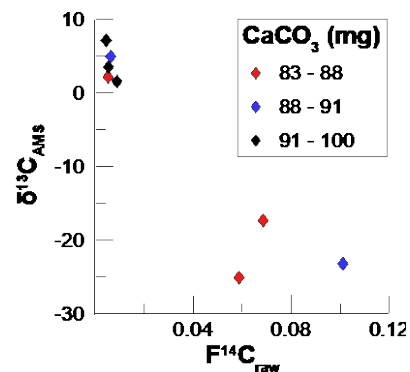
626 **Supplementary Table 2:** All results on ^{14}C measurements on stalagmite WCO extracts.



627

628 **Supplementary Fig 1.:** Comparison between standard and pre-treatment standards after rotary
629 evaporation treatment, showing large offsets from the real value. Chemical pre-treatment
630 standards that were analysed for $\delta^{13}\text{C}$ show large offsets compared to the standards (A –
631 sucrose, B – phthalic acid) due to extraneous carbon introduced by the rotary evaporator.

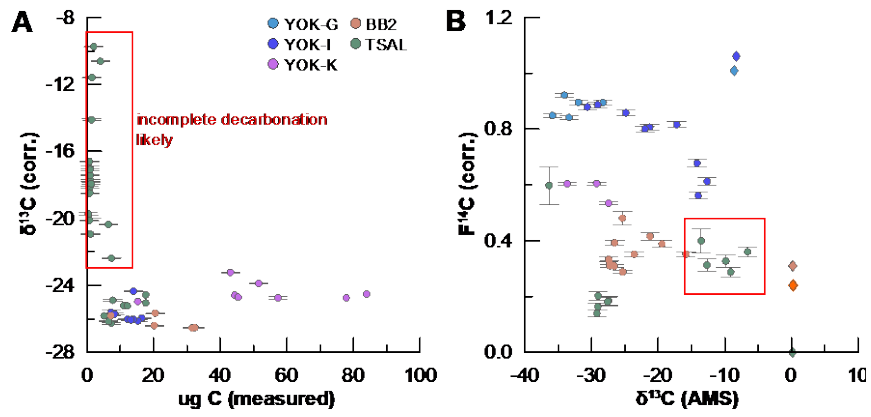
632



633

634 **Supplementary Fig 2.:** Results for vials containing a known amount of IAEA C1 carbonate
635 (^{14}C -dead), spiked with phthalic acid. A weak relationship between sample size and isotopic
636 signature of the WCO is visible, with larger samples showing lower $F^{14}\text{C}$ and less negative $\delta^{13}\text{C}$
637 values, suggesting incomplete decarbonation.

638



639

640 **Supplementary Fig 3.:** Matrix effects resulting in frequent incomplete decarbonation in

641 stalagmite TSAL.